

# Time-tronics: from temporal printed circuit board to quantum computer

Krzysztof Giergiel,<sup>1,2,3</sup> Peter Hannaford,<sup>2</sup> and Krzysztof Sacha<sup>1</sup>

<sup>1</sup>*Instytut Fizyki Teoretycznej, Uniwersytet Jagielloński,  
ulica Profesora Stanisława Łojasiewicza 11, PL-30-348 Kraków, Poland*

<sup>2</sup>*Optical Sciences Centre, Swinburne University of Technology, Melbourne 3122, Australia*

<sup>3</sup>*CSIRO, Manufacturing, Research Way, Clayton, Victoria 3168, Australia*

Time crystalline structures can be created in periodically driven systems [1, 2]. They are temporal lattices which can reveal different condensed matter behaviours ranging from Anderson localization in time to temporal analogues of many-body localization or topological insulators [1, 3]. However, the potential practical applications of time crystalline structures have yet to be explored. Here, we pave the way for time-tronics where temporal lattices are like printed circuit boards for realization of a broad range of quantum devices. The elements of these devices can correspond to structures of dimensions higher than three and can be arbitrarily connected and reconfigured at any moment. Moreover, our approach allows for the construction of a quantum computer, enabling quantum gate operations for all possible pairs of qubits. Our findings indicate that the limitations faced in building devices using conventional spatial crystals can be overcome by adopting crystalline structures in time.

Time crystals, much like their spatial counterparts, spontaneously form through the self-organization of many-body systems but in the time domain [4–7]. In periodically driven systems, discrete time crystals can emerge, evolving spontaneously with a period longer than that dictated by the periodic perturbation [8–26]. In periodically disturbed systems, it is also possible to create time lattices, not resulting from self-organization, but from the application of appropriate temporal resonant perturbations [27–29]. Studies have shown that such time crystalline structures can manifest a wide range of phases known in the physics of condensed matter, such as Anderson localization and many-body localization in time, topological insulators in time, and Mott insulators in the time domain [1, 3, 30].

From the inception of the field of time crystals, questions have arisen regarding how crystalline structures in time can be practically utilized and whether they carry greater potential for practical applications than conventional spatial crystals [1, 2, 23, 31–38]. In this article, we demonstrate that it is possible to achieve time-tronics, where time crystalline structures serve as printed circuit boards as in electronics, allowing the design and realization of a broad range of quantum devices.

We first illustrate how resonantly driven ultra-cold atoms can create a time crystalline structure where the

connection of arbitrary sites through the tunneling of atoms between sites or atom-atom interactions can be realized. As any connections between sites can be controlled, it is possible to realize a broad class of quantum devices, ranging from one-, two-, three- or higher-dimensional structures to more exotic objects like a Klein bottle, all of which can be connected in an arbitrary way, and the entire system can be reconfigured at any time during an experiment.

Next, we focus on a specific example, a quantum computer [39]. We demonstrate that a temporal printed circuit board can host qubits, where all single-qubit operations can be realized and a controlled-Z gate can be performed between all possible qubit pairs, meeting the conditions for a universal quantum computer.

## Temporal printed circuit board

To explain the creation of a time crystalline structure, let us begin with a classical particle moving periodically in a one-dimensional (1D) box between infinite walls. Such a periodic trajectory remains stable in the presence of a periodically oscillating potential if the resonance condition is met, i.e., if the frequency  $\omega$  of the oscillating potential is  $s$  times greater than the frequency of the particle motion, where  $s$  is an integer number [29]. There are  $s$  oscillations of the potential for each period of the particle trajectory, allowing for the simultaneous driving of  $s$  particles that follow each other with a delay  $T = 2\pi/\omega$ , as illustrated in Fig. 1a (see also Methods).

In the quantum realm, this classical system has its close counterpart, where each particle is represented by a localized wave-packet propagating without spreading along the resonant trajectory with a period  $sT$  [1, 29]. In the quantum world, there is the tunneling process that can lead to the transfer of a particle from one wave-packet to neighboring wave-packets. Tunneling times become very long and thus negligible in the experiment if the wave-packets are sufficiently strongly localized. In the following, we assume negligible *natural* tunneling, but we can selectively introduce tunneling between any wave-packets in a controlled manner using Bragg scattering [40], as explained in Fig. 1b (see also Methods). In summary, this allows us to create a system of non-interacting bosons (or fermions) described by the tight-binding model,

$$\hat{H} = \frac{1}{2} \sum_{i,j=1}^s J_{ij} \hat{a}_i^\dagger \hat{a}_j, \quad (1)$$

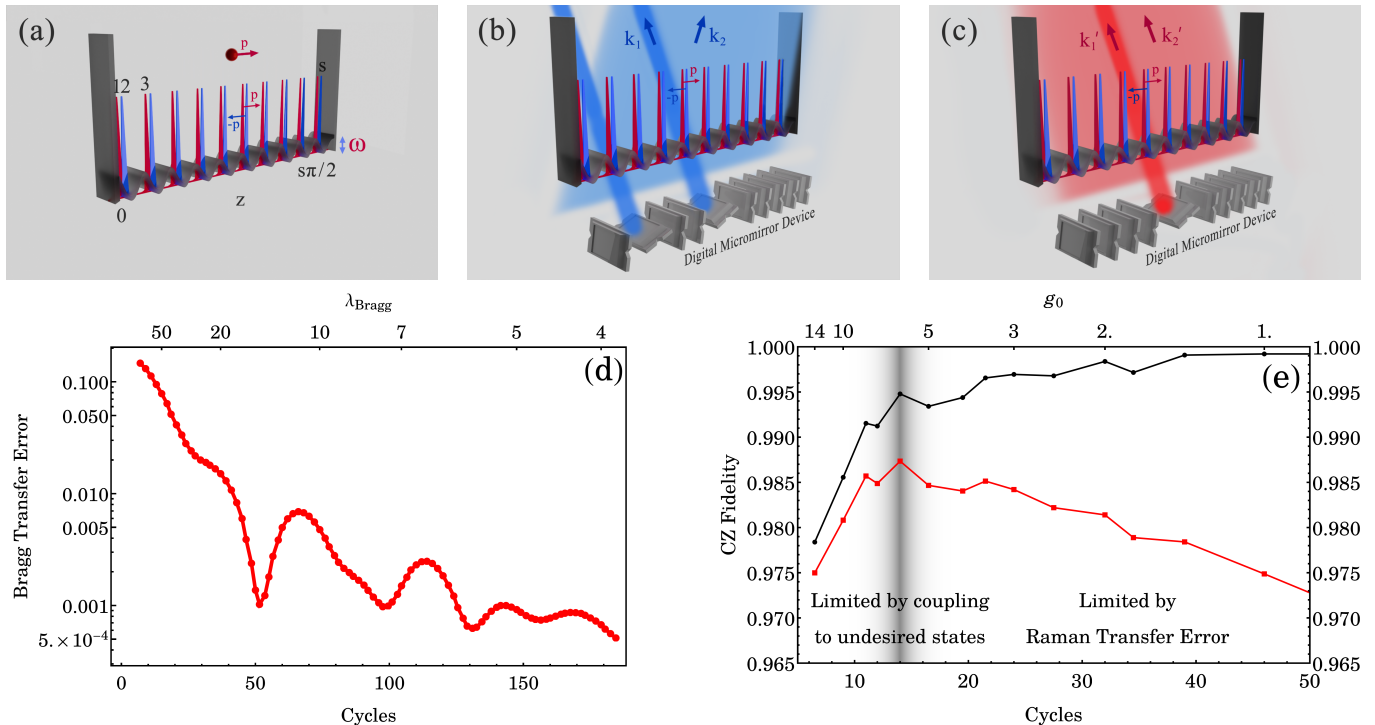


FIG. 1: (a): Red ball illustrates a classical particle moving in a 1D box potential in the presence of an oscillating spatially periodic potential. If the period of particle motion is  $s$  times longer than the period of the oscillating potential,  $T = 2\pi/\omega$ , we have an  $s : 1$  resonance. In such a case,  $s$  classical non-interacting particles can be positioned so that they follow one another along the resonant trajectory. In the quantum description, the  $s : 1$  resonance manifests itself with the presence of  $s$  localized wave-packets, which evolve one after another along the resonant trajectory. A quantum particle prepared in a certain wave-packet can tunnel to neighboring wave-packets. Here, we assume that the wave-packets are sufficiently localized so that *natural* tunneling is negligible. (b): Tunneling can be established in a controlled manner using Bragg scattering [40]. If during the encounter of the  $i$ -th and  $j$ -th wave-packets moving in opposite directions, we briefly turn on one broad laser beam (labelled  $k_2$ ) and one narrow laser beam (labelled  $k_1$ ) focused on the meeting point of the wave-packets and the Bragg condition is satisfied, we can realize atom tunneling between the wave-packets with an amplitude  $J_{ij}$ , the modulus of which depends on the beam parameters and the interaction time with the atom, and a phase depending on the relative phase between the beams. With a controllable array of focused laser beams available (e.g., using a digital micromirror device [41] as sketched in the figure), which can be independently activated at different time points, one can control the tunneling amplitudes  $J_{ij}$  between any pair of wave-packets. (c): Ultra-cold atoms can be prepared in states where they do not interact. In such a situation, we have the possibility of selectively controlling interactions between atoms occupying any pair of wave-packets. If just before the encounter of atoms occupying two wave-packets, we perform a Raman transfer [42] (using broad and focused laser beams) from the initial internal states of the atoms to states where the atoms interact, then during the passage of the wave-packets, interaction between atoms will occur. After the wave-packets pass each other, we perform a Raman transfer again, but back to non-interacting internal states of the atoms. With a digital micromirror device available, interaction between atoms occupying any pair of wave-packets can be realized. (d): Error of atom transfer between two wave-packets using Bragg pulses versus the assumed number of cycles of the resonant trajectory needed to achieve full transfer (two Bragg pulses per each cycle). Faster transfer requires stronger Bragg pulses,  $\lambda_{\text{Bragg}}$ , increasing the coupling of the atom to other undesired states. Generally, apart from additional coherent oscillations, the longer the realization of the transfer, the smaller the error. (e): Fidelity of the controlled-Z gate (CZ), where the interaction imparts a phase of  $\pi$  to the state where one atom occupies one wave-packet and the second atom occupies another wave-packet, versus the number of required cycles (two interaction meetings of the wave-packets per cycle). The two curves represent the cases without (black) and with (red) the inclusion of Raman transfer errors [43] (see Methods). For a small number of cycles, stronger interactions are needed, and the coupling to other states limits the CZ fidelity. For a larger number of cycles, more Raman transfers are needed, and their imperfections limit the fidelity. The results presented in (d) and (e) correspond to  $^{39}\text{K}$  atoms driven resonantly by an optical lattice potential, created by laser radiation with a wavelength  $10.6 \mu\text{m}$ , which oscillates with a frequency  $5.46 \text{ kHz}$  and with Bragg and Raman pulses of wavelength  $266 \text{ nm}$  (see Methods).

where  $\hat{a}_i$  ( $\hat{a}_i^\dagger$ ) represents the bosonic annihilation (creation) operator, responsible for annihilating (creating) a particle in the  $i$ -th wave-packet. All Bragg tunneling amplitudes  $J_{ij}$  are subject to precise control and can be engineered at will at any moment during an experiment. This model describes a crystalline structure in time, or a time lattice. Unlike static states localized in a periodic spatial structure, the lattice sites here correspond to evolving localized wave-packets that form a periodic structure in time (see also Methods).

Initially, we assume non-interacting atoms. This scenario can be realized by means of a Feshbach resonance, i.e., an external magnetic field can be chosen so that the  $s$ -wave scattering length which describes the contact interactions between atoms is zero [44]. The interactions between atoms can then be selectively reinstated, even between atoms occupying different lattice sites in (1), i.e., with  $i \neq j$ . A similar array of laser beams as used for selective Bragg scattering and control of the tunneling amplitudes  $J_{ij}$  can serve this purpose. These laser beams allow for a selective change in the internal state of the atoms by Raman transfer occupying given wave-packets [42]. This change leads to interaction between the atoms when their respective wave-packets intersect during the periodic evolution along the resonant trajectory because the scattering length is no longer zero, as depicted in Fig. 1c. Subsequent to the interaction, the atoms can be reverted to their initial internal state. This approach allows for precise control over interactions between atoms occupying any pair of wave-packets which are characterized by the coefficients  $U_{ij}$  in the Hamiltonian (see Methods)

$$\hat{H} = \frac{1}{2} \sum_{i,j=1}^s \left( J_{ij} \hat{a}_i^\dagger \hat{a}_j + U_{ij} \hat{a}_i^\dagger \hat{a}_j^\dagger \hat{a}_j \hat{a}_i \right). \quad (2)$$

Hence, we have a system in which all tunneling amplitudes  $J_{ij}$  and all interaction coefficients  $U_{ij}$  can be controlled at will at any moment during an experiment.

The Hamiltonian (2) is derived for bosons but a similar universal Hamiltonian can be obtained for fermions. Fermions can be prepared in a time crystalline structure and their tunnelings and interactions can be controlled selectively.

With the universal time crystalline structure described by the Hamiltonian (2), it is possible to realize a broad range of quantum devices. Figure 2a presents a few examples. Physically the states associated with the sites of the time crystalline lattice are localized wave-packets moving periodically in a 1D box (Fig. 1a). One can represent the crystalline structure as a row of sites but if the sites are connected via selective Bragg tunneling as depicted in the middle plot in Fig. 2a, then the structure can be represented as a 2D lattice with nearest neighbor tunnelings, and 2D condensed matter problems can be realized and investigated. For example, fermionic

or bosonic atoms can experience a magnetic-like field if proper complex phases of the tunneling amplitudes  $J_{ij}$  are realized by a proper choice of the relative phase of the laser beams in the Bragg scattering (see Methods). A few such 2D lattices can be created and connected via selective tunneling to form a 3D lattice (bottom plot in Fig. 2a), and this procedure can be continued to form a 4D lattice, and so on. It is also possible to realize exotic objects like a Klein bottle, which is hard to imagine in 3D space. That is, pairs of opposite edges of a 2D lattice can be connected via tunneling, but one of the edges is twisted before the connection.

An entire time crystalline structure can be represented as sites on a 2D board, as shown in Fig. 2b. Such a board can be considered analogous to a printed circuit board in electronics. Indeed, any site on the board can be connected to any other site through selective tunneling, and an atom occupying any site can interact with an atom occupying any other site. All tunnelings and interactions can be individually turned on or off or modified because all parameters of the Hamiltonian (2) are fully controlled. Thus, in one part of the board, we can realize, for example, a 2D structure, while in other parts of the board, there are other 2D or higher-dimensional structures, or a structure with fully connected sites, or even a structure in the form of a Klein bottle. We can realize and control arbitrary connections between the structures and reconfigure the entire system at any moment during the experiment. Consequently, we can realize a broad range of quantum devices that can perform the operations we need.

### Quantum computer

The construction of a universal quantum computer requires the preparation of numerous qubits (e.g., two-level atoms), the ability to perform all single-qubit operations, and the capability to execute two-qubit operations (e.g., controlled-Z gate operation) between any pairs of qubits [39]. The latter necessitates selective interactions between atoms, which, in turn, demand precise coherent transport of atoms and activation of interactions when they are in close proximity [43, 47, 48].

Crystalline structures in time automatically address the atom transport problem, as atoms are prepared in wave-packets evolving along a periodic trajectory, and each atom individually encounters every other atom at some point in time. Additionally, every atom moving on the same trajectory means they experience the same low frequency spatially inhomogeneous fields, thus likely reducing phase noise sources. To realize a controlled-Z gate for any pair of atoms, it is sufficient to activate interactions between them at the moment of their encounter. The temporal printed circuit board described in the previous section is well-suited for this purpose. The board also enables the implementation of all necessary single-qubit operations required for building a quantum computer. For the successful construction of a quantum

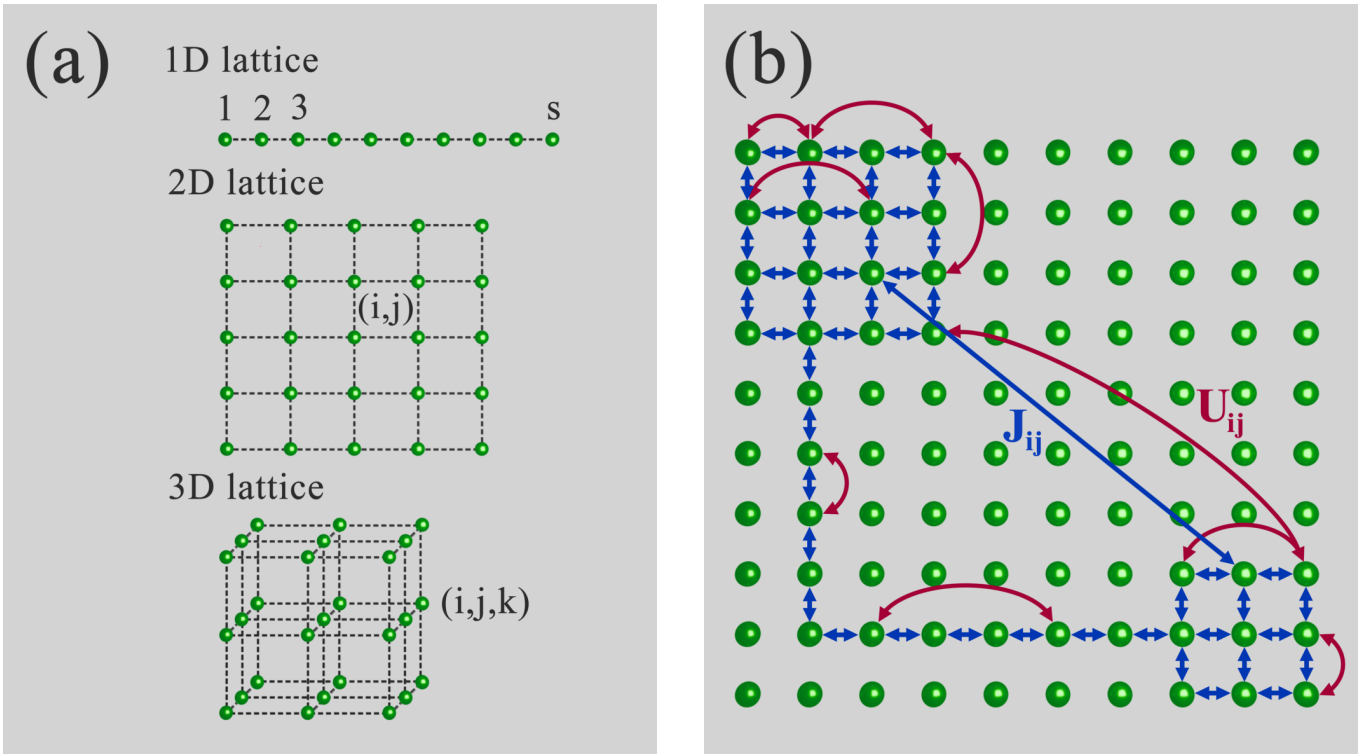


FIG. 2: **Temporal printed circuit board.** (a): The  $s$  wave-packets evolving along the resonant trajectory (Fig. 1a) can be treated as  $s$  states of a lattice with  $s$  sites. If we arrange the sites of the lattice in a 1D chain and using Bragg scattering (Fig. 1b) we realize tunneling between nearest neighbors, we will have a 1D crystalline structure with nearest neighbor hoppings. If we arrange the sites in a 2D lattice and tunneling between nearest neighbors, we will have a 2D crystalline structure. Similarly, we can realize 3D and higher-dimensional crystalline structures. (b): Let us consider  $s$  periodically evolving wave-packets as states of a 2D lattice. Using a broad laser beam and having only two focused laser beams at our disposal (Fig. 1b), all nearest neighbor tunnelings of the 2D lattice can be realized. For example, a 2D sublattice can be coupled to another 2D sublattice via a 1D chain as shown in the figure (realized tunnelings are marked with blue arrows). Control over the phases of tunneling amplitudes  $J_{ij}$  allows for the generation of an artificial magnetic field in the system. With an array of focused laser beams available, any sites in the lattice can be connected via tunneling, as illustrated by the long blue arrow. More exotic geometries can also be realized, such as the Klein bottle, where the left and right edges of the 2D lattice are connected normally, but the top edge is twisted before connection to the bottom edge. Using selective Raman transfer (Fig. 1c), interactions between atoms occupying any pair of sites can be realized and controlled (as indicated by red arched arrows in the plot). During an experiment, the entire system can undergo any reconfiguration.

computer, all gate operations need to be as straightforward as possible. In the proposed approach, which we describe in the following, we only need a static arrangement of focused laser beams that will be activated at the appropriate moments, allowing the implementation of all necessary gate operations.

The crystalline structure in time, as described in Fig. 1, consists of  $s$  states ( $s$  localized wave-packets). In such a structure, if we prepare  $s/2$  atoms, we can define  $s/2$  qubits, assigning two different wave-packets to each atom (see Fig. 3). If the atom occupies the first chosen wave-packet, the qubit will be in the state  $|1\rangle$  and if it occupies the second wave-packet, it will be in the state  $|0\rangle$ . The initialization process of all qubits in, for example, state  $|1\rangle$  is relatively straightforward. In the 1D box potential and in the presence of a static deep optical lattice, we prepare bosons in a Mott insulator state with unit filling of

lattice sites [44], assuming the number of lattice sites between the walls of the box potential is  $s/2$  (see Methods). Next, we turn off the interactions between atoms setting the  $s$ -wave scattering to zero by means of a Feshbach resonance [44]. We then kick the atoms so that they start moving in one direction with momentum  $p$  that satisfies the  $s : 1$  resonance condition with the frequency of the optical lattice oscillation and activate the optical lattice oscillation. This leads to a situation where  $s/2$  wave-packets of the time crystalline structure that are initially moving in the same direction are occupied by individual atoms, while the other  $s/2$  wave-packets initially moving in the opposite direction are unoccupied, see Fig. 3a and Methods. For each occupied wave-packet, we assign any unoccupied wave-packet to form a qubit together. The choice of which unoccupied wave-packets are assigned to which occupied wave-packets is arbitrary.

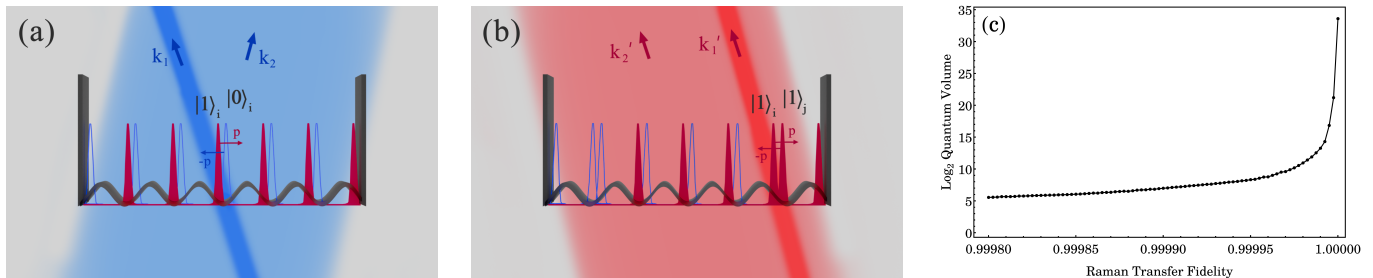


FIG. 3: **Quantum computer.** (a): Initially,  $s/2$  bosonic atoms are prepared in a Mott insulator phase in a 1D box potential in the presence of a static optical lattice. We assume there are  $s/2$  potential wells in the box, with one atom in each well. After preparing the Mott insulator phase, the interactions between atoms are turned off by means of a Feshbach resonance [44]. The next step is to impart a kick to the atoms, so that they start moving with momenta that satisfy the  $s : 1$  resonance condition with the frequency of the optical lattice oscillation, which we simultaneously switch on. Shortly after the previously described procedure, we observe  $s/2$  wave-packets occupied by single atoms moving to the right in the figure and  $s/2$  unoccupied wave-packets moving to the left. We assign one unoccupied wave-packet to each occupied wave-packet, forming the  $|0\rangle$  and  $|1\rangle$  states of qubits. In total, we have  $s/2$  qubits. When two wave-packets corresponding to the  $|0\rangle$  and  $|1\rangle$  states of the same qubit meet during evolution along the resonant trajectory, a single-qubit gate can be performed using Bragg scattering. Control over the relative phase of the laser beams used in the Bragg scattering allows us to control whether the  $\sigma_x$  or  $\sigma_y$  operation is performed. High fidelity single-qubit operations are achieved by dividing them into several stages, meaning the entire single operation requires multiple encounters of wave-packets, and hence spanning several periods of the resonant trajectory (Fig. 1d). (b): When wave-packets corresponding to the states  $|1\rangle_i$  and  $|1\rangle_j$  of the  $i$ -th and  $j$ -th qubits meet during evolution, a controlled-Z gate can be realized. Atoms initially do not interact, but just before the wave-packets pass each other, we change the internal states of the atoms to states where they interact. We do this using Raman transfer with two beams. After passing each other, another Raman transfer restores the initial internal states of the atoms. If the interaction strength between atoms and the duration of interaction are appropriately chosen, after the wave-packets pass, the state  $|1\rangle_i|1\rangle_j$  acquires a phase  $e^{i\pi}$ , and the controlled-Z gate is completed. Similarly to single-qubit operations, a high fidelity controlled-Z gate can be realized by dividing it into several encounters of the appropriate wave-packets (Fig. 1e). (c): Quantum volume [45] calculated based on the B-gate decomposition of a generic  $SU(4)$  two-qubit operation [46]. In this plot we assume no error in the single qubit operations. We plot a square of fidelity of decomposition of a single B-gate using optimal points selected from the CZ-fidelity plot (Fig. 1e). For the higher the Raman transfer fidelity one can use a longer multi-cycle realization of the CZ-gates leading to quick increase in the quantum volume. The results correspond to the same parameters as in Figs. 1d-1e.

If we want to perform  $\sigma_x$  or  $\sigma_y$  operations on a selected qubit, we have to wait for the moment when two wave-packets corresponding to the given qubit meet during the evolution along the periodic trajectory. At that moment, we activate the appropriate focused laser beam along with a second broad laser beam, allowing Bragg scattering and thus the transfer of an atom from one wave-packet moving with momentum  $p$  to another wave-packet moving with momentum  $-p$ , or vice versa (Fig. 3a). Phase control between the laser beams allows choosing whether the transfer corresponds to  $\sigma_x$  or  $\sigma_y$  operations, the composition of which enables the realization of  $\sigma_z$  operations. Very high fidelity of single-qubit operations is achieved if the full transfer of atoms between wave-packets is divided into a few encounters (see Fig. 1d and Methods). The period of the resonant trajectory can be regarded as a single clock cycle of the quantum processor. This means that a few cycles of the processor clock are needed to perform high-fidelity single-qubit operations.

So far, we have assumed that the atoms do not interact. Interaction arises if we change the internal state of the atoms. The previously described focused laser beams allow for the local activation of interactions between atoms when the wave-packets they occupy meet during the evo-

lution along the periodic trajectory. This enables us to implement a controlled-Z gate between any pair of qubits.

Let us assume that one atom occupies the wave-packet corresponding to the state  $|1\rangle$  of a certain qubit, and another atom occupies the wave-packet corresponding to the state  $|1\rangle$  of another qubit. Just before the moment when these two wave-packets meet, we can change the internal state of one or both atoms by activating the appropriate focused laser beams together with the broad laser beam, causing Raman transitions and altering the internal state of the atoms (Fig. 3b). Then, during the passage of the wave-packets, the atoms interact. Immediately after the passage, we use laser beams again to restore the atoms to their initial internal states, in which there are no interactions. If the interaction energy is properly chosen, a phase imprint of  $e^{i\pi}$  occurs during the interaction. Such a phase imprint only occurs when both qubits are in the  $|1\rangle$  states, thus implementing the controlled-Z gate. For all qubits whose wave-packets corresponding to the  $|1\rangle$  states meet at the same moment, controlled-Z gate operations can be carried out in parallel. In subsequent periods of the oscillation of the optical lattice potential, a controlled-Z gate can be performed for other pairs of qubits whose wave-packets

corresponding to the  $|1\rangle$  states meet at different moments in time. To achieve high-fidelity controlled-Z gates, the entire gate operation needs to be divided into a few encounters of wave-packets (Fig. 1e), i.e., a few clock cycles of the quantum processor are necessary. The ability to perform two-qubit operations between all qubits makes a key parameter of quantum computing, i.e., quantum volume [45], achieve very high values, especially when the Raman transfer error is reduced (Fig. 3c).

It is worth emphasizing that even with only a few focused laser beams, we can perform a network of quantum operations that are challenging to achieve in other experimental setups. A single beam focused in one location is sufficient to execute all necessary single-qubit operations, but in this case, the qubits must be associated with wave-packets that meet at the focus point of the beam. The addition of a second beam focused in another location allows the implementation of a controlled-Z gate between the nearest neighboring qubits that can be arranged in a 1D chain. If we introduce yet another focused beam, we gain the capability to perform controlled-Z gates between nearest neighboring qubits that can be arranged in a square network. A fourth beam enables controlled-Z gates between the nearest neighboring qubits arranged in a 3D cube, and so on.

### Discussion and outlook

Periodically perturbed systems can give rise to crystalline structures in time, which, in the time domain, exhibit phenomena similar to those known in traditional spatial crystals [1]. In this study, we demonstrate that time crystalline structures possess significant potential for practical applications. In conventional spatial structures, various components of the system are spatially separated, and selective communication and interaction between distant parts of the system are preceded by their spatial transport. In time crystalline structures, the transport problem is automatically resolved because wave-packets associated with sites of time lattices evolve periodically in time, naturally encountering each other at different time instances. This opens up the possibility of creating any temporal printed circuit board capable of implementing a wide range of quantum devices for bosons or fermions. Similar to electronics, this gives rise to the field of time-tronics. What is a formidable challenge in spatial structures becomes trivial in temporal structures. As a concrete example, we describe the implementation of a universal quantum computer, in which the key problem of qubit transport [43, 47] for realizing two-qubit gates between any pair of qubits is automatically addressed.

In this article, we present a detailed realization of a temporal printed circuit board and a quantum computer in a system of atoms moving periodically in a box potential. An advantage of such a potential is that all gate operations are performed in the same manner, regardless of where in space the atoms meet. However, a temporal printed circuit board and a quantum computer can also

be implemented when atoms move in different potentials. In such cases, the parameters of gate operations should be appropriately chosen depending on where in space the atoms meet. This opens up the possibility of developing time-tronics in a broad class of ultra-cold atomic gas laboratories.

## METHODS

### Time crystalline structure

Consider a single atom confined within a 1D box potential periodically perturbed by an oscillating optical lattice potential (Fig. 1a). Using units for length, energy, and time, denoted as  $1/k$ ,  $\hbar^2 k^2/m$ , and  $m/\hbar k^2$ , respectively, where  $k$  is the wave number of the laser beam creating the oscillating optical lattice potential, and  $m$  is the mass of the atom, the system Hamiltonian is given by

$$H_0 = \frac{p^2}{2} + \frac{\lambda}{2} \cos^2(z) + \frac{\lambda}{2} \cos^2(z) \cos(\omega t), \quad (3)$$

where  $\lambda$  and  $\omega$  represent the amplitude and frequency of the oscillating optical lattice potential, and  $z$  ranges from 0 to the size of the box,  $L = s\pi/2$ , where  $s$  is an integer. In the classical description, if the driving frequency is  $s$  times larger than the frequency of the unperturbed motion of the atom, i.e.,  $\omega = s|p|\pi/L = 2|p|$ , where the resonant momentum  $|p| \gg \sqrt{\lambda}$ , the condition for the  $s : 1$  resonance is met [29]. For a given optical lattice potential (i.e., for a selected wavelength of the laser beam,  $2\pi/k$ ), the resonant number  $s$  depends on the size of the 1D box potential. By increasing the size of the 1D box, we can achieve any value of  $s$ .

Before considering the quantum resonant behavior of the atom, let us commence with a classical description. We introduce a new pair of momentum and position variables, known as action-angle variables [29],  $I = s|p|/2$  and  $|\theta| = 2z/s$  where  $-\pi \leq \theta < \pi$ . Switching to the moving frame,  $\Theta = \theta - \omega t/s$ , and neglecting rapidly oscillating terms, the effective Hamiltonian becomes  $H_{\text{eff}} = P^2/2 + (\lambda s^2/32) \cos(s\Theta)$ , where  $P = I - \omega/s$  [1, 29]. For  $s \gg 1$ ,  $H_{\text{eff}}$  describes an atom moving in a spatially periodic potential. In the quantum description, this results in solid-state-like behavior, which is manifested as the formation of energy bands and eigenstates in the form of Bloch waves [1, 30].

Upon returning from the moving frame to the laboratory frame, this solid-state-like behavior is observed in the time domain [1]. Indeed, when fixing the position in space ( $\theta = \text{const}$ ) in the laboratory frame and examining how the probability of observing the atom at a chosen point changes in time, this replicates the crystalline structure observed versus  $\Theta$  in the moving frame. This is due to the linear time transformation between the laboratory and moving frames, i.e.,  $\Theta = \theta - \omega t/s$ . This concept

has facilitated the exploration of various condensed matter phases in the time domain across different resonantly driven single-particle and many-body systems [1, 3].

In the main text, we confine our focus to the lowest energy band of the quantum version of the Hamiltonian  $H_{\text{eff}}$ . The corresponding Hilbert subspace can be expanded in the Wannier state basis,  $w_i(\Theta)$ , where  $w_i(\Theta)$  is localized at the  $i$ -th site of the potential in  $H_{\text{eff}}$  [1, 3]. In the laboratory frame, these are localized wave-packets,  $w_i(z, t)$ , evolving along the periodic resonant trajectory with the resonant momentum  $p$ , i.e., with the period  $sT$ , where  $T = 2\pi/\omega$  (Fig. 1a). In this basis, the Hamiltonian of many non-interacting atoms takes the form (1), where  $J_{ij} = -2 \int_0^L dz, w_i^*(H_0 - i\partial_t)w_j$  represents the tunneling amplitudes of atoms between the wave-packets [1, 49]. We set  $\lambda$  such that these *natural* tunnelings are negligible, as our intention is to selectively introduce tunneling through Bragg scattering in a controlled manner.

#### Control of the tunneling amplitudes $J_{ij}$

To selectively control atom transfer between different wave-packets, we can utilize Bragg scattering [40]. Let us consider two laser beams characterized by wave vectors  $\mathbf{k}_1$  and  $\mathbf{k}_2$  that we switch on for a short period of time  $\tau$ . The first beam is focused at the location where two wave-packets,  $w_i(z, t)$  and  $w_j(z, t)$ , meet during evolution (Figs. 1a, 3a). The waist of the beam is larger than the width of the wave-packets but smaller than the distance between potential minima in (3). The second beam is broad and covers the entire 1D box. If the Bragg condition is satisfied,  $\mathbf{k}_1 - \mathbf{k}_2 = 2p\mathbf{e}_z$ , an atom occupying the wave-packet  $w_j$ , moving with an average momentum  $p\mathbf{e}_z$ , is transferred to the other wave-packet  $w_i$  which moves with an average momentum  $-p\mathbf{e}_z$ , and the reverse transfer is equally probable. These processes are described by an additional term in the Hamiltonian [40]

$$H_B = \lambda_{\text{Bragg}} \cos^2 \left[ \frac{(\mathbf{k}_1 - \mathbf{k}_2) \cdot \mathbf{e}_z z + \phi}{2} \right] \frac{e^{-\frac{(z-z_0)^2}{W^2}}}{\sqrt{4\pi W^2}}, \quad (4)$$

where  $z_0$  and  $W$  are the location and waist of the narrow laser beam, respectively. We choose  $W = \pi/(2\sqrt{2})$ .  $\lambda_{\text{Bragg}}$  is determined by the intensities of the beams and  $\phi$  is the relative phase of the beams. The resulting tunneling amplitude of the atom between the wave-packets is described by  $J_{ij} = -2 \int_t^{t+\tau} dt \int_0^L dz w_i^* H_B w_j$ . The magnitude of  $J_{ij}$  is controlled by the parameters of the beams and the duration of their interaction with the atom (we choose  $\tau = 0.24T$ , where  $T = 2\pi/\omega$ , around central moments of wave-packet encounters), while the phase is controlled by the relative phase  $\phi$ . By switching on the beams during meetings of different wave-packets and having multiple focused beams available, we have the ability to control the transfer of atoms between all wave-packets (Fig. 2), i.e., we can realize the Hamiltonian (1).

As an example of a concrete realization of the system, let us consider  $^{39}\text{K}$  atoms confined in a 1D box

potential and subjected to an oscillating optical lattice potential created by  $\text{CO}_2$  laser radiation with a wavelength of  $10.6 \mu\text{m}$ . We assume that the 1D confinement is achieved using a strong harmonic trapping potential with a transverse confinement frequency of the order of  $\omega_{\perp} = 2\pi \times 100 \text{ kHz}$ . The oscillation of the optical lattice has an amplitude of  $\lambda = 30$  (60 recoil energies) and a frequency of  $\omega = 60$  ( $2\pi \times 5.46 \text{ kHz}$ ). The *natural* tunneling is very weak, requiring more than  $10^6$  cycles of the driving force to transfer the atom between neighboring wave-packets. However, Bragg scattering can significantly reduce this time. By employing two laser beams with a wavelength of  $266 \text{ nm}$  (and a waist of the focused beam of  $1.9 \mu\text{m}$ ) propagating at angles  $\pm 46^\circ$  with respect to the  $z$ -axis, atom transfer between any wave-packets can be completed within a few meetings of the wave-packets along the resonant trajectory. Figure 1d illustrates the efficacy of such transfers. Faster transfers necessitate stronger Bragg pulses (i.e., larger  $\lambda_{\text{Bragg}}$ ), leading to unwanted coupling with other states of the system. Decreasing the intensity of the Bragg lasers reduces the error, but there is a critical point where the error starts increasing due to the effectiveness of the *natural* tunneling.

#### Control of the interaction strengths $U_{ij}$

Interactions between ultra-cold atoms are effectively short-range contact interactions described by a single parameter, the s-wave scattering length [44]. In the Hilbert subspace spanned by the wave-packets,  $w_i(z, t)$ , evolving along the periodic resonant trajectory, the interaction coefficients in the Hamiltonian (2) read [1, 49]

$$U_{ij} = g_0 \int_0^L dz |w_i(z, t)|^2 |w_j(z, t)|^2, \quad (5)$$

with  $g_0 = 2m\omega_{\perp}a/\hbar k$ , where  $a$  is the scattering length. Let us consider bosonic atoms where, choosing properly an external magnetic field in the vicinity of a Feshbach resonance [44], we set the scattering length  $a = 0$ . If we change the internal state of the atoms that occupy two wave-packets which are about to meet during the evolution along the periodic trajectory, they will interact because the scattering length  $a$  is no longer zero. The change of the internal state can be performed by a focused laser beam which together with another broad beam realizes a Raman transition of the atoms between the internal states [42] (Figs. 1c, 3b). Immediately after the wave-packets pass each other, the laser beams can be applied once again to restore the initial internal states of the atoms. The entire procedure leads to a time-dependent  $g_0(t)$  in (5) which is non-zero only during the passing of the wave-packets. With an array of focused laser beams one can control and engineer all interaction coefficients  $U_{ij}$  in the Hamiltonian (2), see Fig. 2b.

For  $^{39}\text{K}$  atoms, which we are using as an example here, the s-wave scattering length can be set to zero if the atoms are initially prepared in the hyperfine state  $|1, +1\rangle$

and the magnetic field is set to the zero crossing value of 350.5 G, close to the Feshbach resonance at 402.5 G [50, 51]. However, if we transfer the atoms to the state  $|1, -1\rangle$ , which is 213 MHz above the  $|1, +1\rangle$  state, using a Raman pulse, the corresponding scattering length becomes  $-29$  Bohr radii, and the interaction coefficient (5) does not vanish. By varying the frequencies  $\omega_{\perp}$  of the harmonic trap in the transverse directions (i.e., choosing different values of  $g_0$ ), we can analyze how many meetings of the two wave-packets are needed to imprint a  $\pi$  phase in the state in which each of the two atoms occupies one of the wave-packets. Simultaneously, we can determine the fidelity of the process, which is the probability that the atoms remain in their initially occupied wave-packets. The results of this analysis are presented in Fig. 1e. They correspond to  $\omega_{\perp}/2\pi$  in the range between 50 kHz and 700 kHz.

### Quantum computer

Suppose that bosonic atoms are prepared in a Mott insulator state in a static optical lattice potential [44], i.e.,  $\omega = 0$  and  $\lambda = 7.5$  in (3). We assume that the number of atoms is equal to the number of lattice sites in the box potential, i.e.,  $s/2$  (Fig. 3), i.e., there is one atom in each potential well. After preparing the Mott insulator phase, we adjust the s-wave scattering length to zero using the Feshbach resonance as described in the preceding paragraph. We also kick the atoms so that they start moving in the same direction with momentum  $p$  and activate resonant oscillations of the optical lattice with frequency  $\omega = 2|p| = 60$  and amplitude  $\lambda = 30$ . As a result, we have  $s/2$  wave-packets occupied by single atoms, which start moving with average momentum  $p$  along the resonant trajectory corresponding to the  $s : 1$  resonance. At the same time, the remaining  $s/2$  resonant wave-packets which are not occupied by atoms start moving with average momentum  $-p$ . Now we can associate the states of  $s/2$  qubits with wave-packets. We assign one occupied wave-packet and one unoccupied wave-packet to each qubit. For example, occupied wave-packets will be called states  $|1\rangle$ , and unoccupied wave-packets will be called states  $|0\rangle$  of the qubits. With this convention, initially, we have all qubits prepared in the state  $|1\rangle$ .

When the wave-packets corresponding to the states  $|0\rangle$  and  $|1\rangle$  of the same qubit meet during evolution along the resonant trajectory, Bragg scattering allows for  $\sigma_x$  or  $\sigma_y$  single-qubit operations depending on the relative phase  $\phi$  between the broad laser beam and the beam focused at the meeting point of the wave packets (Fig. 3a). Figure 1d presents the fidelity of the single-qubit gates for the system of  $^{39}\text{K}$  atoms which we consider as an example here. A single focused laser beam (together with a broad beam) is sufficient to perform single-qubit operations for all qubits if the qubit states are assigned so that the wave-packets corresponding to  $|0\rangle_i$  and  $|1\rangle_i$  pass each other at different moments of time but at the same location for all  $i$ , i.e., all qubits. On the other hand, if

multiple focused laser beams are available, the appropriate assignment allows for parallel single-qubit operations.

To implement a controlled-Z gate for the  $i$ -th and  $j$ -th qubits, we need to wait until the wave-packets corresponding to the states  $|1\rangle_i$  and  $|1\rangle_j$  of those qubits meet during evolution along the resonant trajectory. Just before their meeting, we briefly turn on the broad laser beam and the laser beam focused at the location of the wave-packets, which induce Raman transfer to the internal states of the atoms where the atoms interact [42] (Fig. 3b). After the wave-packets pass each other, the Raman laser beams are briefly turned on again, causing the atoms to return to their initial non-interacting internal states. If the interaction strength and the duration of the interaction are properly chosen, after the wave-packets pass each other, the state  $|1\rangle_i|1\rangle_j$  acquires a phase  $e^{i\pi}$  and a controlled-Z gate is realized. To minimize coupling of the wave-packets with other states during the interaction, i.e., to achieve high fidelity of the gate, it is necessary to divide the gate implementation into multiple encounters of the wave-packets (Fig. 1e).

For the  $^{39}\text{K}$  atoms under consideration and for the fidelity,  $F_R = 0.999933$ , achieved in the Raman transfer in Ref. [43], the optimal fidelity of the controlled-Z gate is 0.987 which requires 14 cycles of the resonant trajectory (Fig. 1e). The fidelity was determined by multiplying the fidelity obtained assuming perfect Raman transfers (black curve in Fig. 1e) by  $F_R^{8n}$ , where the  $8n$  comes from the fact that for each of  $n = 14$  cycles two interactions take place where two atoms are transferred twice by Raman pulses. Higher fidelity of the gate can be achieved either by improving  $F_R$  or by increasing the frequency of the optical lattice oscillation  $\omega$ . A higher  $\omega$  allows for a greater oscillation amplitude  $\lambda$ , thereby enabling the use of stronger interactions without undesired couplings to other states of the system. Stronger interactions facilitate imprinting the  $\pi$  phase onto states with high fidelity in fewer cycles of the resonant trajectory, thereby reducing the impact of imperfect Raman transfers.

A significant advantage of the proposed quantum computer is the ability to perform two-qubit gates between any pair of qubits. This is quantitatively illustrated by the quantum volume presented in Fig. 3c. In the example we consider here and for the Raman transfer fidelity achieved in Ref. [43],  $F_R = 0.999933$ , and for 49 cycle single-qubit gates (cf. Fig. 1d), a system of 7 qubits is capable of executing universal quantum operations.

### Acknowledgements

This research was funded by the National Science Centre, Poland, Project No. 2021/42/A/ST2/00017 and Australian Research Council Discovery Project Grants DP190100815 and DP240101590. We acknowledge Michał Grabowski for preparing the graphics.



- 
- [1] K. Sacha, *Time Crystals* (Springer International Publishing, Switzerland, Cham, 2020), ISBN 978-3-030-52523-1, URL <https://doi.org/10.1007/978-3-030-52523-1>.
- [2] M. P. Zaletel, M. Lukin, C. Monroe, C. Nayak, F. Wilczek, and N. Y. Yao, *Rev. Mod. Phys.* **95**, 031001 (2023), URL <https://link.aps.org/doi/10.1103/RevModPhys.95.031001>.
- [3] P. Hannaford and K. Sacha, *Association of Asia Pacific Physical Societies Bulletin* **32**, 12 (2022), 2202.05544.
- [4] F. Wilczek, *Phys. Rev. Lett.* **109**, 160401 (2012), URL <http://link.aps.org/doi/10.1103/PhysRevLett.109.160401>.
- [5] P. Bruno, *Phys. Rev. Lett.* **111**, 070402 (2013), URL <http://link.aps.org/doi/10.1103/PhysRevLett.111.070402>.
- [6] H. Watanabe and M. Oshikawa, *Phys. Rev. Lett.* **114**, 251603 (2015), URL <http://link.aps.org/doi/10.1103/PhysRevLett.114.251603>.
- [7] V. K. Kozin and O. Kyriienko, *Phys. Rev. Lett.* **123**, 210602 (2019), URL <https://link.aps.org/doi/10.1103/PhysRevLett.123.210602>.
- [8] K. Sacha, *Phys. Rev. A* **91**, 033617 (2015), URL <http://link.aps.org/doi/10.1103/PhysRevA.91.033617>.
- [9] V. Khemani, A. Lazarides, R. Moessner, and S. L. Sondhi, *Phys. Rev. Lett.* **116**, 250401 (2016), URL <http://link.aps.org/doi/10.1103/PhysRevLett.116.250401>.
- [10] D. V. Else, B. Bauer, and C. Nayak, *Phys. Rev. Lett.* **117**, 090402 (2016), URL <http://link.aps.org/doi/10.1103/PhysRevLett.117.090402>.
- [11] J. Zhang, P. W. Hess, A. Kyprianidis, P. Becker, A. Lee, J. Smith, G. Pagano, I.-D. Potirniche, A. C. Potter, A. Vishwanath, et al., *Nature* **543**, 217 (2017), ISSN 0028-0836, URL <http://dx.doi.org/10.1038/nature21413>.
- [12] S. Choi, J. Choi, R. Landig, G. Kucsko, H. Zhou, J. Isoya, F. Jelezko, S. Onoda, H. Sumiya, V. Khemani, et al., *Nature* **543**, 221 (2017), ISSN 0028-0836, URL <http://dx.doi.org/10.1038/nature21426>.
- [13] S. Pal, N. Nishad, T. S. Mahesh, and G. J. Sreejith, *Phys. Rev. Lett.* **120**, 180602 (2018), URL <https://link.aps.org/doi/10.1103/PhysRevLett.120.180602>.
- [14] J. Rovny, R. L. Blum, and S. E. Barrett, *Phys. Rev. Lett.* **120**, 180603 (2018), URL <https://link.aps.org/doi/10.1103/PhysRevLett.120.180603>.
- [15] J. Smits, L. Liao, H. T. C. Stoof, and P. van der Straten, *Phys. Rev. Lett.* **121**, 185301 (2018), URL <https://link.aps.org/doi/10.1103/PhysRevLett.121.185301>.
- [16] X. Mi, M. Ippoliti, C. Quintana, A. Greene, Z. Chen, J. Gross, F. Arute, K. Arya, J. Atalaya, R. Babbush, et al., *Nature* **601**, 531 (2022), ISSN 1476-4687, URL <https://doi.org/10.1038/s41586-021-04257-w>.
- [17] J. Randall, C. E. Bradley, F. V. van der Grienden, A. Galicia, M. H. Abobeih, M. Markham, D. J. Twitchen, F. Machado, N. Y. Yao, and T. H. Taminiiau, *Science* **374**, 1474 (2021), 2107.00736.
- [18] P. Frey and S. Rachel, *Science Advances* **8**, eabm7652 (2022), <https://www.science.org/doi/pdf/10.1126/sciadv.abm7652>, URL <https://www.science.org/doi/abs/10.1126/sciadv.abm7652>.
- [19] H. Keßler, P. Kongkhambut, C. Georges, L. Mathey, J. G. Cosme, and A. Hemmerich, *Phys. Rev. Lett.* **127**, 043602 (2021), URL <https://link.aps.org/doi/10.1103/PhysRevLett.127.043602>.
- [20] A. Kyprianidis, F. Machado, W. Morong, P. Becker, K. S. Collins, D. V. Else, L. Feng, P. W. Hess, C. Nayak, G. Pagano, et al., *Science* **372**, 1192 (2021).
- [21] H. Xu, J. Zhang, J. Han, Z. Li, G. Xue, W. Liu, Y. Jin, and H. Yu (2021), arXiv:2108.00942.
- [22] H. Taheri, A. B. Matsko, L. Maleki, and K. Sacha, *Nature Communications* **13**, 848 (2022), ISSN 2041-1723, URL <https://doi.org/10.1038/s41467-022-28462-x>.
- [23] Z. Bao, S. Xu, Z. Song, K. Wang, L. Xiang, Z. Zhu, J. Chen, F. Jin, X. Zhu, Y. Gao, et al., arXiv e-prints arXiv:2401.08284 (2024), 2401.08284.
- [24] K. Shinjo, K. Seki, T. Shirakawa, R.-Y. Sun, and S. Yunoki, arXiv e-prints arXiv:2403.16718 (2024), 2403.16718.
- [25] B. Liu, L.-H. Zhang, Z.-K. Liu, J. Zhang, Z.-Y. Zhang, S.-Y. Shao, Q. Li, H.-C. Chen, Y. Ma, T.-Y. Han, et al., arXiv e-prints arXiv:2402.13657 (2024), 2402.13657.
- [26] B. Liu, L.-H. Zhang, Y. Ma, T.-Y. Han, Q.-F. Wang, J. Zhang, Z.-Y. Zhang, S.-Y. Shao, Q. Li, H.-C. Chen, et al., arXiv e-prints arXiv:2404.12180 (2024), 2404.12180.
- [27] L. Guo, M. Marthaler, and G. Schön, *Phys. Rev. Lett.* **111**, 205303 (2013), URL <https://link.aps.org/doi/10.1103/PhysRevLett.111.205303>.
- [28] K. Sacha, *Sci. Rep.* **5**, 10787 (2015), URL <https://www.nature.com/articles/srep10787>.
- [29] A. Buchleitner, D. Delande, and J. Zakrzewski, *Physics reports* **368**, 409 (2002), URL <http://www.sciencedirect.com/science/article/pii/S0370157302002703>.
- [30] L. Guo, *Phase Space Crystals*, 2053-2563 (IOP Publishing, 2021), ISBN 978-0-7503-3563-8, URL <https://dx.doi.org/10.1088/978-0-7503-3563-8>.
- [31] P. Hannaford and K. Sacha, *Europhysics Letters* **139**, 10001 (2022), URL <https://dx.doi.org/10.1209/0295-5075/ac796d>.
- [32] R. W. Bomantara and J. Gong, *Phys. Rev. Lett.* **120**, 230405 (2018), URL <https://link.aps.org/doi/10.1103/PhysRevLett.120.230405>.
- [33] M. P. Estarellas, T. Osada, V. M. Bastidas, B. Renoust, K. Sanaka, W. J. Munro, and K. Nemoto, *Sci. Adv.* **6**, eaay8892 (2020).
- [34] F. Carollo, K. Brandner, and I. Lesanovsky, *Phys. Rev. Lett.* **125**, 240602 (2020).
- [35] C. Lyu, S. Choudhury, C. Lv, Y. Yan, and Q. Zhou, *Phys. Rev. Res.* **2**, 033070 (2020), URL <https://link.aps.org/doi/10.1103/PhysRevResearch.2.033070>.
- [36] F. Iemini, R. Fazio, and A. Sanpera, arXiv:2306.03927 (2023).
- [37] V. Montenegro, M. G. Genoni, A. Bayat, and M. G. Paris, *Commun. Phys.* **6**, 304 (2023).
- [38] R. Yousefjani, K. Sacha, and A. Bayat, arXiv e-prints arXiv:2405.00328 (2024), 2405.00328.
- [39] J. Preskill, *Quantum* **2**, 79 (2018), ISSN 2521-327X, URL <https://doi.org/10.22331/q-2018-08-06-79>.
- [40] H. Müller, S.-w. Chiow, and S. Chu, *Phys. Rev. A* **77**, 023609 (2008), URL <https://link.aps.org/doi/10.1103/PhysRevA.77.023609>.
- [41] Y. Wang, S. Shevate, T. M. Wintermantel, M. Morgado, G. Lochead, and S. Whitlock, *npj Quantum Information*

- 6**, 54 (2020), ISSN 2056-6387, URL <https://doi.org/10.1038/s41534-020-0285-1>.
- [42] H. Levine, D. Bluvstein, A. Keesling, T. T. Wang, S. Ebadi, G. Semeghini, A. Omran, M. Greiner, V. Vuletić, and M. D. Lukin, *Phys. Rev. A* **105**, 032618 (2022), URL <https://link.aps.org/doi/10.1103/PhysRevA.105.032618>.
- [43] D. Bluvstein, H. Levine, G. Semeghini, T. T. Wang, S. Ebadi, M. Kalinowski, A. Keesling, N. Maskara, H. Pichler, M. Greiner, et al., *Nature* **604**, 451 (2022), ISSN 1476-4687, URL <https://doi.org/10.1038/s41586-022-04592-6>.
- [44] C. Pethick and H. Smith, *Bose-Einstein condensation in dilute gases* (Cambridge University Press, Cambridge, England, 2002).
- [45] A. W. Cross, L. S. Bishop, S. Sheldon, P. D. Nation, and J. M. Gambetta, *Physical Review A* (2018), URL <https://api.semanticscholar.org/CorpusID:119408990>.
- [46] J. Zhang, J. Vala, S. Sastry, and K. B. Whaley, *Physical review letters* **93** **2**, 020502 (2003), URL <https://api.semanticscholar.org/CorpusID:9632700>.
- [47] J. I. Cirac and P. Zoller, *Nature* **404**, 579 (2000), ISSN 1476-4687, URL <https://doi.org/10.1038/35007021>.
- [48] D. González-Cuadra, D. Bluvstein, M. Kalinowski, R. Kaubruegger, N. Maskara, P. Naldesi, T. V. Zache, A. M. Kaufman, M. D. Lukin, H. Pichler, et al., *Proc Natl Acad Sci U S A* **120**, e2304294120 (2023).
- [49] J. Wang, K. Sacha, P. Hannaford, and B. J. Dalton, *Phys. Rev. A* **104**, 053327 (2021), URL <https://link.aps.org/doi/10.1103/PhysRevA.104.053327>.
- [50] C. D’Errico, M. Zaccanti, M. Fattori, G. Roati, M. Inguscio, G. Modugno, and A. Simoni, *New Journal of Physics* **9**, 223 (2007), URL <https://dx.doi.org/10.1088/1367-2630/9/7/223>.
- [51] K. Giergiel, T. Tran, A. Zaheer, A. Singh, A. Sidorov, K. Sacha, and P. Hannaford, *New Journal of Physics* **22**, 085004 (2020), URL <https://doi.org/10.1088/1367-2630/aba3e6>.